Multi-layer thermoelectric-temperature-mapping microbial incubator designed for geo-biochemistry applications

Jin-Gen Wu,[1] Man-Chi Liu,[1] Ming-Fei Tsai,[1] Wei-Shun Yu,[1] Jian-Zhang Chen,[2,a)]
I-Chun Cheng,[3] and Pei-Chun Lin[1,a)]
[1]*Department of Mechanical Engineering, National Taiwan University, Taipei 10617, Taiwan*
[2]*Institute of Applied Mechanics, National Taiwan University, Taipei 10617, Taiwan*
[3]*Department of Electrical Engineering & Graduate Institute of Photonics and Optoelectronics, National Taiwan University, Taipei 10617, Taiwan*

(Received 7 November 2011; accepted 8 April 2012; published online 26 April 2012)

We demonstrate a novel, vertical temperature-mapping incubator utilizing eight layers of thermoelectric (TE) modules mounted around a test tube. The temperature at each layer of the TE module is individually controlled to simulate the vertical temperature profile of geo-temperature variations with depth. Owing to the constraint of non-intrusion to the filled geo-samples, the temperature on the tube wall is adopted for measurement feedback. The design considerations for the incubator include spatial arrangement of the energy transfer mechanism, heating capacity of the TE modules, minimum required sample amount for follow-up instrumental or chemical analysis, and the constraint of non-intrusion to the geo-samples during incubation. The performance of the incubator is experimentally evaluated with two tube conditions and under four preset temperature profiles. Test tubes are either empty or filled with quartz sand, which has comparable thermal properties to the materials in the geo-environment. The applied temperature profiles include uniform, constant temperature gradient, monotonic-increasing parabolic, and parabolic. The temperature on the tube wall can be controlled between 20 °C and 90 °C with an averaged root mean squared error of 1 °C. © *2012 American Institute of Physics*. [http://dx.doi.org/10.1063/1.4705748]

I. INTRODUCTION

Thermoelectric (TE) modules are advantageous in their practical controllability of bi-directional heat conduction. By simply adjusting the direction and magnitude of current flowing through the TE modules, heating and cooling functions of the TE modules can be generated. This bi-directional heat conduction feature greatly benefits the implementation of the temperature feedback control apparatus. The alternative application of the TE modules is power generation, with a temperature difference applied across the module. Regarding either temperature control or power generation, the TE modules have been applied in many scientific and technological aspects,[1] including direct contact platform for capillary columns,[2] vapor pressure measurements,[3] single-molecule atomic force microscopy measurements,[4] the fluid stage for atomic force microscopy,[5] the thermostat for precision optical radiation measurements,[6] the cryosurgery device,[7] nuclear magnetic resonance sample temperature control,[8] across-wafer temperature uniformity control in photoresist processing,[9] the wireless pulse oximeter for non-invasive measurement of pulse and blood oxygen saturation,[10] the laser-stabilizing stage,[11] and thermocapillary droplet actuation microfluidic chips,[12] etc. In this study, we use TE modules to construct a miniaturized apparatus to simulate the temperature profiles of geological environments where the microbial habitats situate.

Functions and activity of living organisms are highly related to environmental factors. In extreme geological environments, temperature appears to govern critically the distribution, population, and structures of microbial habitats.[13–15] One typical example is the aerobic and anaerobic oxidation of methane.[16,17] Continental shield regions have a steady thermal structure with a geothermal gradient ranging from 5 to 15 °C/km.[18] In some extreme geo-environments, thermal gradients can be much larger, and the extent of microbial habitats is greatly reduced. In hot springs, the thermal gradients can be as high as 0.1 °C/m,[19] and they can be even higher in mud volcanos (~3 °C/m).[20] Thus, researchers are interested in studying geological microbial activity that is under the influence of temperature gradients or non-linear thermal maps. A thermal mapping system must be designed that can adjust the temperature profiles for a microbial incubator, allowing the interchange of microbes and microbial activity products between different temperature layers in real geological systems.

Because of interests in microbial community evolution at various temperatures, several research reports have used temperature gradient incubators (TGIs) for studying microorganism activity and seed germination.[21–23] More complex biochemical reactions also have been monitored using TGIs, such as the occurrence of alterations with fatty acids of *Saccharomyces cerevisiae* under extreme growth temperatures.[24] There is some variety in the design of TGIs by placing test tubes in a large, constant thermal gradient block with cooling and heating elements on both sides.[22,25] All these designs involve merely a constant temperature gradient with one heating and one cooling unit on the two ends of the incubator. The

a)Authors to whom correspondence should be addressed. Electronic addresses: peichunlin@ntu.edu.tw and jchen@ntu.edu.tw.

temperature profile between the heating and cooling ends cannot be altered, and the microorganisms inside each test tube are exposed in a single designated temperature.

In this paper, we demonstrate a novel, vertical temperature-mapping incubator using eight layers of TE modules mounted around a test tube. The temperature at each layer of the TE module can be individually manipulated and controlled. We can then simulate the vertical temperature profile of a designated geo-temperature variation in one test tube. Thus, the microbes and microbial activity products can freely move between various temperature layers. The incubator is suitable for studying microbial ecosystems to monitor the microbial habitat and activity product distribution at a designed temperature profile.

Section II describes the incubator design and implementation, including the concept design of the system, system realization, and mechatronic setup. Section III reports the experimental evaluation and discussion of the system. Section IV concludes the work.

II. INCUBATOR DESIGN AND IMPLEMENTATION

A. Design of the incubator

Our goal is to develop an incubator capable of heating or cooling different portions of a test tube with different temperature settings. Because commercially available regular borosilicate glass tubes are generally long and thin, our strategy is to create an environment with the temperature varied in the longitude direction of the tube. In this arrangement, the installation of multiple heating sources for fine temperature adjustment around the tube is feasible, and the temperature profile in the test tube can be approximated as one dimensional in the longitude direction (i.e., the temperature variation in the radial direction can be ignored). Eight heating sources along the longitude direction of the tube are adopted in the empirical setup, providing eight independent temperature controls (hereafter referred to as eight "layers"). The TE modules are utilized as the heating sources because of their bi-directional heat flow controllability. The heating and cooling functions can be manipulated simply by adjusting the direction and magnitude of electric current flowing through the TE modules. To effectively conduct heat in and out the test tube in each layer, one side of the TE module surface (i.e., the inner surface) is adhered to an aluminum ring that clamps the tube, and the other side (i.e., the outer surface) is mounted to an aluminum heat sink for thermal energy dissipation. In addition, an aluminum ring is installed between the TE modules and the test tube for three purposes: (i) to act as the structure of the incubator, (ii) to distribute the thermal energy around the tube evenly, and (iii) to interface the round surface of the test tube and flat surface of the TE module. The illustrative drawing of the incubator is depicted in Fig. 1(a).

B. Implementation of the incubator

The empirical implementation of each layer of the incubator is shown in Fig. 1(b). Because a circular, hollow TE module with a designated diameter is not commercially available, eight rectangular TE modules with dimensions of 15 mm × 15 mm × 3.6 mm (TES1-031.30, Tande Energy and Temperature Associates PTY. Co.) are utilized as the heating source and are arranged octagonally around the test tube. The wires of the eight modules are serially connected such that the heating or cooling functions of the modules can be simultaneously employed by applying a single voltage source. The outer surface of each TE module is mounted with a heat sink for heat dissipation. Because of the octagonal arrangement of

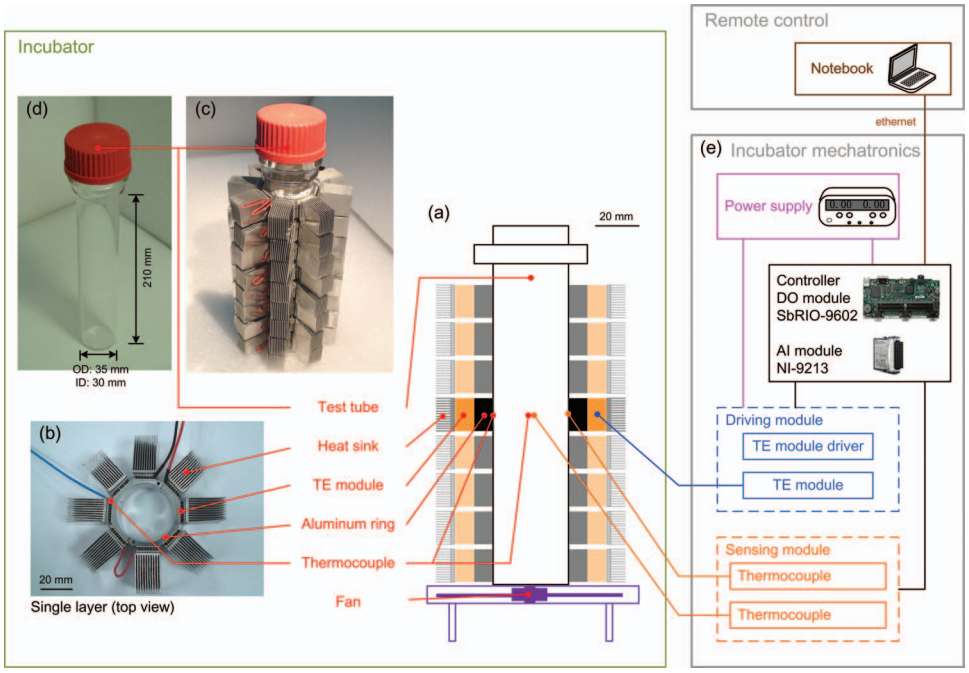

FIG. 1. Illustration of the incubator and the control system: (a) illustrative drawing of the incubator; (b) top view of the single layer; (c) photo of the incubator; (d) photo of the test tube; (e) sketch of the control system.

the TE modules, the outer surface of the aluminum ring is shaped octagonally, and the inner surface is shaped circularly to surround the test tube. The inner diameter of the aluminum ring is 36 mm, which is 1 mm larger than the nominal diameter of the test tube to provide the tolerance for dimension variation. Thermal pastes (i.e., silicone heat sink compound, EG-150, Electrolube) are used to reduce the thermal resistance at the aluminum/tube interface. To facilitate the installation and removal of the test tube, the aluminum ring is composed of two half-rings that can be quickly jointed together or dissembled into two pieces. A small hole is drilled in the aluminum ring to house the thermocouple for *in situ* temperature measurements. In this fashion, the heating and sensory mechanisms are established separately in each layer.

A photo of the incubator is shown in Fig. 1(c), which is composed of a test tube and eight layers of eight serially connected TE modules. The eight layers are stacked vertically. To prevent the thermal disturbance between the adjacent layers, O-rings with a 3 mm height are used between layers of TE modules. Together with a 17-mm-height aluminum ring, the height of each layer is 20 mm. Thus, the height of the incubator with thermal regulation capability is 160 mm. The test tube is placed inside the stacking layers, shown in Fig. 1(d). It is composed of a 35-mm-diameter borosilicate glass tube (PYREX) and GL-45 Polypropylene screwed cap, thus achieving an anaerobic environment for microbial incubation. Please note that if the sealing of the sample is not crucial, a commercial and ordinary borosilicate glass tube can be used directly. A cooling fan is installed beneath the whole incubator to improve the convection of the heat sink fins to the ambient air. The dimension of the fan is selected to match the size of the heat sink so that the forced airflow mainly goes through the heat sink and has little thermal effect on the test tube. Because all layers can be activated individually and simultaneously for heating or cooling, the temperature profile of the test tube can be actively modulated through the temperature control of these eight layers.

C. Mechatronics

Temperature control of the eight layers around the test tube is achieved by a mechatronic system; the layout of the whole system is depicted in Fig. 1(e). A 400-MHz real-time SbRIO-9602 (National Instruments) embedded system is utilized as the main computer, which has onboard digital output (DO) channels ready for interfacing the TE modules. For each layer, the DO signals are connected to one commercial VNH3SP30 (STMicroelectronics) driver chip that has an internal H-bridge circuit; thus, the direction and magnitude of the current into the TE module can be controlled by the pulse width modulation method (i.e., the mechanism is equivalent to adjusting the direction and amount of the heat flux crossing two surfaces of the TE cooler). The temperature of the aluminum ring (or the surface of the test tube) is measured by a thermocouple in real time, and the signal is sent to the SbRIO-9602 embedded system via a NI-9213 (National Instruments) thermocouple input module. With the implemented sensory and driving systems, the temperature of each layer is controllable by an ordinary PID control strategy. The data acquisition, controller, and graphic user interface are programmed using LabVIEW 2009 (National Instruments) with a 2-Hz sampling rate. The PID controller and data acquisition through NI-9213 (i.e., two LabVIEW sub VIs) are programmed based on the sample codes provided by National Instruments. The user interface is customized for this particular application. In the final program, the temperature profiles for the test tube (i.e., the designated temperatures of eight layers) can be pre-programmed into the embedded system SbRIO-9602 or remotely controlled by the operator via standard Ethernet or wireless protocols.

III. SYSTEM PERFORMANCE EVALUATION AND DISCUSSION

Thermal cycle performance for a single layer of TE modules mounted on the empty test tube is shown in Fig. 2. The temperature was programmed to modulate between 15 °C and 100 °C with a 10.4-min period, including transition to the preset temperature and steady-state control at the preset temperature. The means and standard deviations (STDs, shown in parentheses) of the 15 °C to 100 °C and 100 °C to 15 °C transient times are 0.96(0.03) min and 1.80(0.06) min, respectively. Small STDs indicate the controllability of the system and repeatability of performance. Because the operation of TE modules also generates heat, as expected, the 15 °C to 100 °C transient time is faster than the 100 °C to 15 °C transient time. The means and STDs (shown in parentheses) of the root mean squared (RMS) errors of the controlled 15 °C and 100 °C temperatures in all cycles are 0.8(0.1) °C and 1.1(0.2) °C, respectively. Similarly, small STDs indicate the controllability of the system and repeatability of performance.

The performance of the incubator in the benchmark test with the empty tube is shown in Fig. 3 and Table I, where all eight layers are set to the same temperatures ranging from 20 °C to 90 °C with a 10 °C increment (i.e., eight sets of experiments). The incubator was tested in ordinary lab condition without any special environmental treatment to keep the ambient temperature conditions more stable. The averaged temperature readings of eight layers in eight sets of experimental runs are individually plotted in Fig. 3. After the system is activated, the temperatures of all layers transit from room temperature to the preset temperature. The means and STDs

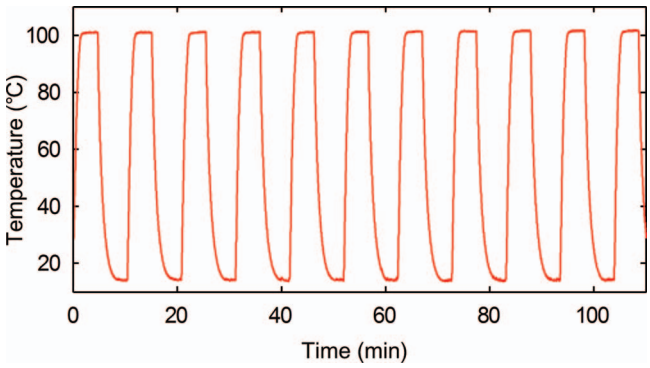

FIG. 2. Thermal cycle test of a single-layer TE module.

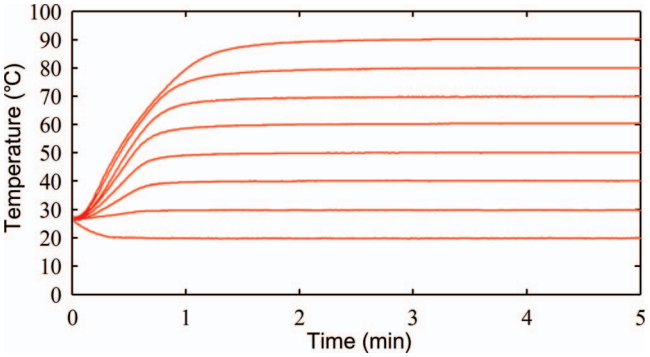

FIG. 3. Temperature profiles of the benchmark tests where all eight layers are set to the same temperatures (from 20 °C up to 90 °C with a 10 °C increment). The averaged temperature readings among the eight layers in all eight sets of experimental runs are plotted. The associated statistic data are reported in Table I.

of transient time of eight layers in eight sets of experimental runs are separately listed in Table I. The transient time is defined as the time within which the system transits from 10% to 90% preset temperature from room temperature. The averaged transient times are all less than 1 min. As expected, the averaged transient time increases as the setting temperature increases because more energy is required for the incubator. In addition, because of the consistency of the heating characteristics, the transient curves are overlapped, as shown in Fig. 3. After the transition, the system reaches the preset temperature and is controlled to maintain at this temperature. The steady-state performance of the system is evaluated by the RMS error between the preset and actual temperatures. The means and STDs of the RMS steady-state temperature errors of eight layers in eight sets of experimental runs are listed separately in Table I. The means of the RMS errors in all eight sets of experiments are less than or equal to 0.4 °C (averaged 0.3 °C), which confirms controllability of the system temperature ranging from 20 °C to 90 °C. In addition, the STDs of the RMS errors among all eight layers in all eight sets of experiments are less than or equal to 0.2 °C, which confirms the performance consistency among layers.

Figure 4 (a, empty tube; b, filled with quartz sand) demonstrates the capability of the incubator to simulate a constant temperature gradient from 20 °C (at the lowest layer) to 90 °C (at the highest layer). The mathematical relation between height, h (unit: cm), and preset temperature, T_p (unit: °C), is $T_p = (h + 30)/2$. The associated statistic data are reported in Table II, including transient time, t_t (unit: min), and RMS steady-state temperature error, T_R (unit: °C). Figure 4(a) plots the measured temperatures of the empty test tube. Figure 4(a-1) shows the temperature transient from the

TABLE I. Performance of the incubator with uniform temperature profile.

	Transient time (min)		Steady-state RMS error (°C)	
Temp (°C)	Mean	STD	Mean	STD
20	0.33	0.08	0.4	0.2
30	0.58	0.03	0.2	0.1
40	0.53	0.05	0.2	0.1
50	0.55	0.03	0.1	0.0
60	0.60	0.05	0.4	0.2
70	0.68	0.05	0.3	0.1
80	0.80	0.08	0.3	0.1
90	0.97	0.08	0.4	0.0

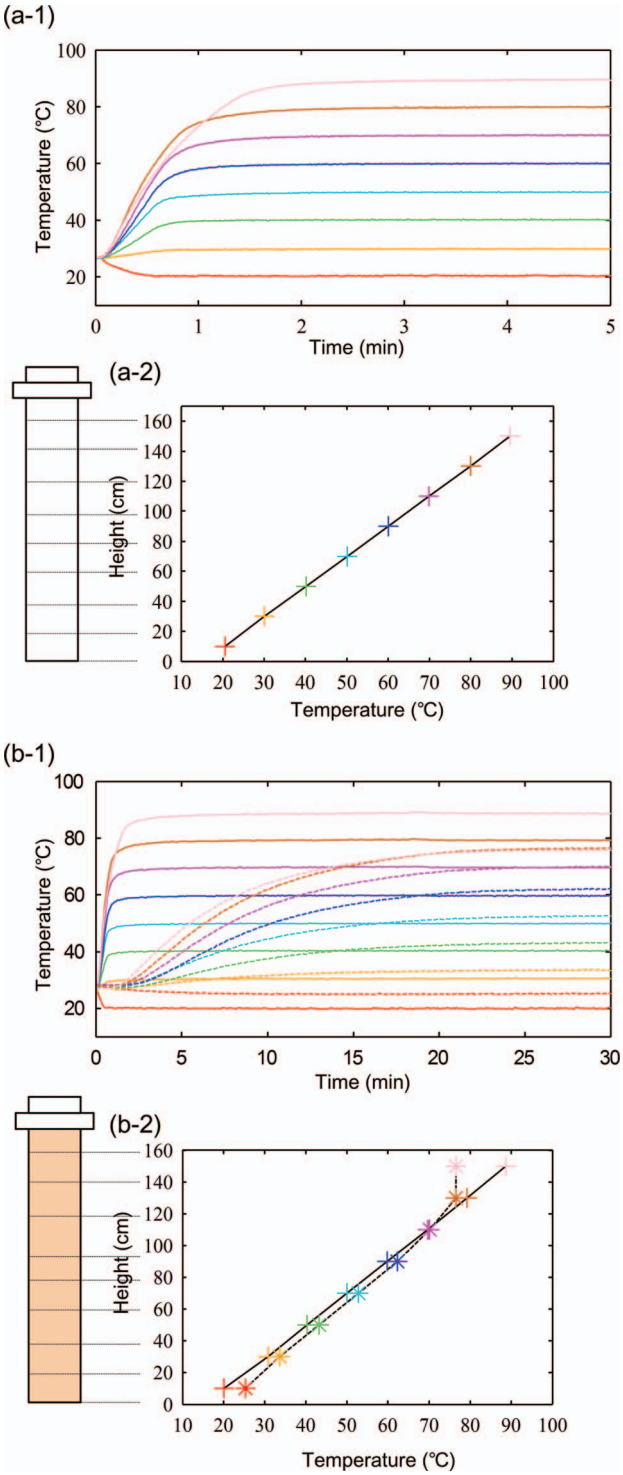

FIG. 4. Experiment with constant temperature gradient profile: (a) empty tube; (b) tube filled with quartz sand. The figures (−1) plot the temperature transient profiles for each layer, where temperatures at the tube surfaces and the centers are plotted in solid and dashed curves, respectively. The figures (−2) show steady-state temperatures of all layers, where temperatures at the tube surfaces and the centers are marked as cross (+) and star (*), respectively. The associated statistic data are reported in Table II.

TABLE II. Performance of the incubator with constant-gradient temperature profile.

			Empty tube		Tube filled with quartz sand			
					Tube surface		Tube center	
Layer	h (cm)	T_p (°C)	t_t (min)	T_R (°C)	t_t (min)	T_R (°C)	t_t (min)	T_R (°C)
8	150	90	1.22	1.0	1.42	1.4	12.8	14.3
7	130	80	0.87	0.5	0.92	0.8	13.5	3.6
6	110	70	0.77	0.3	0.83	0.3	13.6	0.2
5	90	60	0.67	0.2	0.75	0.3	13.7	2.0
4	70	50	0.59	0.2	0.74	0.1	18.8	2.5
3	50	40	0.53	0.2	0.67	0.4	12.1	3.1
2	30	30	0.68	0.2	1.83	0.5	13.8	3.5
1	10	20	0.33	0.5	0.33	0.1	5.17	5.2

TABLE III. Performance of the incubator with monotonic-increasing parabolic temperature profile.

			Empty tube		Tube filled with quartz sand			
					Tube surface		Tube center	
Layer	h (cm)	T_p (°C)	t_t (s)	T_R (°C)	t_t (s)	T_R (°C)	t_t (s)	T_R (°C)
8	150	27	1.97	0.3	2.59	0.9	15.3	10.1
7	130	60	0.66	0.5	0.67	1.2	14.0	2.3
6	110	70	0.73	0.2	1.08	1.1	14.3	1.5
5	90	77	0.78	0.3	1.08	1.3	14.1	1.4
4	70	83	0.90	0.4	1.08	2.1	14.2	1.2
3	50	87	1.01	0.4	1.33	2.2	14.3	0.4
2	30	88	1.00	0.6	1.25	2.6	13.3	1.1
1	10	90	1.07	0.6	1.33	2.2	13.2	1.8

initial conditions to the set temperatures for all eight layers. Although the preset temperatures in all layers are not identical as in the experiments shown in Fig. 3, the transient times from the room temperature to the preset temperatures are basically similar to those shown in Fig. 3, which confirms the control independency among layers. Figure 4(a-2) plots the corresponding steady-state temperatures of all layers. As shown in Table II, the lower seven layers exhibit temperature linearity with RMS errors less than or equal to 0.5 °C (averaged 0.3 °C), whereas the top layer shows 1 °C because of heat loss from the cap. When the test tube is filled with sand or mud from the geo-environment, the temperature at the tube center is different from that on the tube surface because of horizontal and vertical heat transfers by the filling. Figure 4(b) plots the measured temperatures at the center (dashed curves) and on the surface (solid curves) of the test tube filled with 50-μm-diameter dry quartz sand (Rich Sou Co.), which has comparable heat transfer properties to the materials in the geo-environment. In Fig. 4, subplot (b-1) shows the temperature transient behavior, and subplot (b-2) depicts the comparison of the preset and measured temperatures. Because of extra heat transfer to the filling, the transient times of the temperatures on the tube wall with filling are 32.9% more than on the tube wall without filling (i.e., empty tube), as shown in Table II. In the present design, because the tube wall temperatures are utilized for sensory feedback, several system characteristics can be observed: (i) After the tube surfaces reach the preset temperatures, the amount of energy transfer in/out the tube is limited because the boundary condition of the tube surface is altered from the heat source to the fixed temperature. (ii) Together with the slow thermal response of the filling (i.e., thermal diffusivity is around 1.4×10^{-6} m^2/s), the temperatures at the center require an extra 12.0 min on average to reach the steady states, as shown in Fig. 4(b-1). (iii) Because of the vertical heat loss along the tube, the RMS steady-state temperature error at the tube center of the lower seven layers (shown in Fig. 4(b-2)) is on average 2.9 °C, which is larger than that at the tube wall (0.34 °C). The relative larger discrepancy of 14.3 °C at the top layer is a result of the edge heat transfer through the tube cap.

Figure 5 (a, empty tube; b, filled with quartz sand) demonstrates the capability of the incubator to simulate a monotonic-increasing parabolic temperature profile, whereas Fig. 6 (a, empty tube; b, filled with quartz sand) demonstrates the capability of the incubator to simulate a parabolic temperature profile. The mathematical relations between height, h (unit: cm), and preset temperature, T_p (unit: °C), in these two figures are $T_p = \sqrt{-18.2h + 2910} + 40.9$ and $T_p = 0.014h^2 - 2.3h + 107$, respectively. The associated statistic data are reported in Tables III and IV, accordingly, including transient time, t_t (unit: min), and RMS steady-state temperature error, T_R (unit: °C). Similarly, subplot (−1) of Fig. 5 shows the temperature transient behavior and subplot (−2) depicts the comparison of the preset and measured temperatures. Although the temperature profiles in these two experiments are more dramatic than those in the constant temperature gradient case shown in Fig. 4, the trends of the results are similar. First, top and/or bottom layers also exhibit the edge heat transfer phenomenon. Second, ignoring the layers with edge heat transfer, the surface temperatures for the empty tube can be controlled with an averaged RMS error of 0.4 °C in the monotonic-increasing parabolic case and 0.5 °C in the parabolic case. In addition, the RMS errors of those for the filled tube are 1.8 °C and 1.0 °C, respectively. Next, transient times of the temperatures at the tube center are larger than those on the tube wall and are also determined by both horizontal and vertical heat transfers. For the profiles with smaller temperature differences between the adjacent layers, the effect of vertical heat transfer is less; therefore, the temperature difference between the tube surface and center mainly results from heat

TABLE IV. Performance of the incubator with parabolic temperature profile.

			Empty tube		Tube filled with quartz sand			
					Tube surface		Tube center	
Layer	h (cm)	T_p (°C)	t_t (s)	T_R (°C)	t_t (s)	T_R (°C)	t_t (s)	T_R (°C)
8	150	88	1.35	0.7	1.42	1.3	13.3	16.9
7	130	50	0.69	0.2	1.00	0.3	54.5	4.5
6	110	29	2.13	0.8	5.08	2.0	36.2	7.2
5	90	21	0.52	0.6	0.43	0.8	25.9	5.0
4	70	20	0.55	0.3	0.43	0.6	22.4	2.4
3	50	29	0.64	0.5	5.78	1.4	29.0	0.1
2	30	49	0.62	0.4	0.85	0.7	44.7	4.3
1	10	88	1.67	1.5	1.92	1.3	12.0	21.3

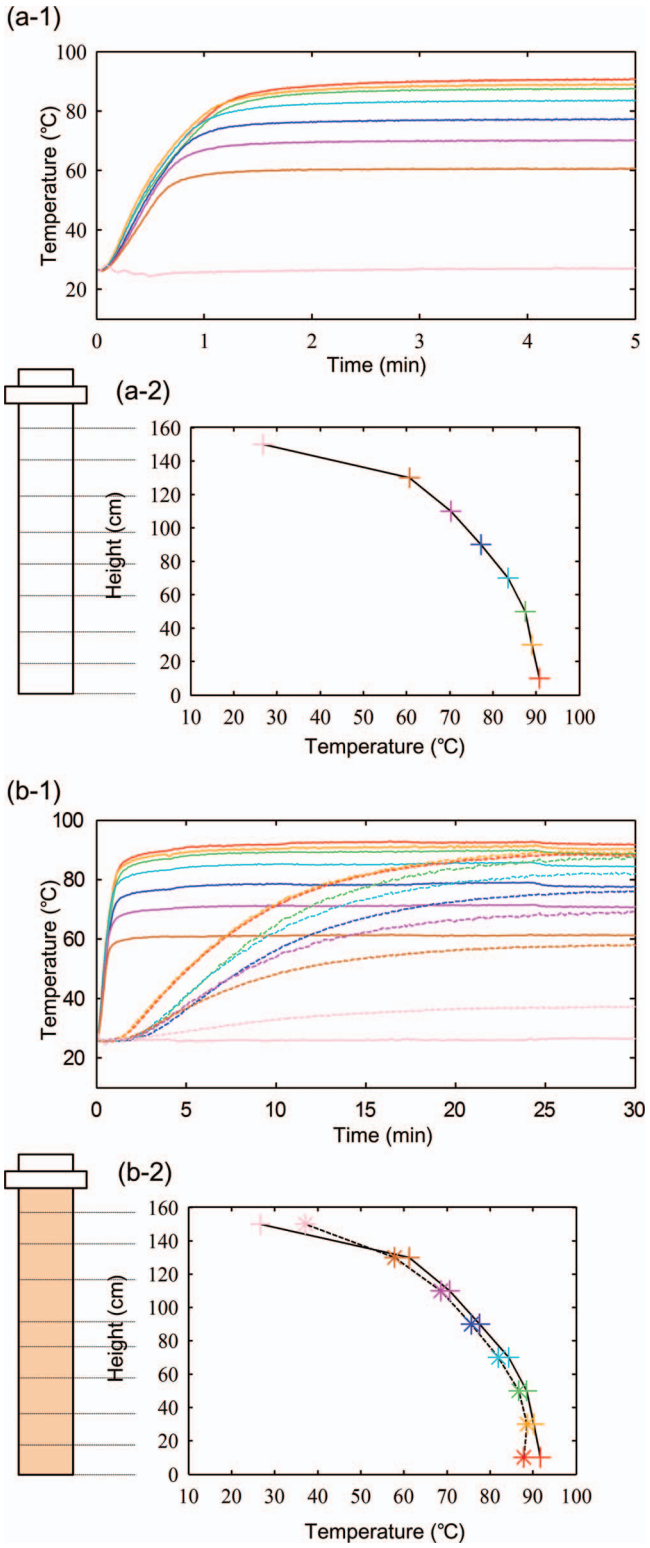

FIG. 5. Experiment with monotonic-increasing parabolic temperature profile: (a) empty tube; (b) tube filled with quartz sand. The figures (−1) plot the temperature transient profiles for each layer, where temperatures at the tube surfaces and the centers are plotted in solid and dashed curves, respectively. The figures (−2) show steady-state temperatures of all layers, where temperatures at the tube surfaces and the centers are marked as cross (+) and star (*), respectively. The associated statistic data are reported in Table III.

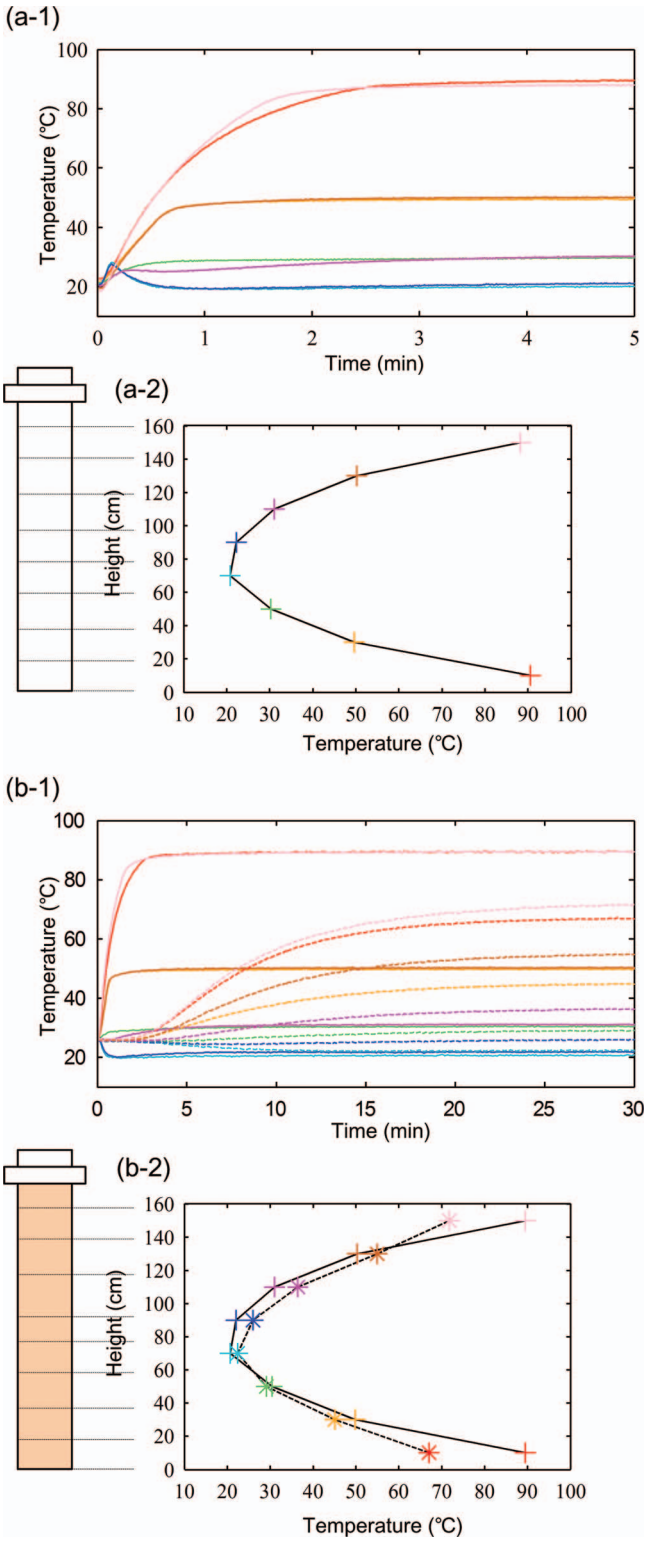

FIG. 6. Experiment with parabolic temperature profile: (a) empty tube; (b) tube filled with quartz sand. The figures (−1) plot the temperature transient profiles for each layer, where temperatures at the tube surfaces and the centers are plotted in solid and dashed curves, respectively. The figures (−2) show steady-state temperatures of all layers, where temperatures at the tube surfaces and the centers are marked as cross (+) and star (*), respectively. The associated statistic data are reported in Table IV.

transfer in the horizontal direction. With a "fixed" temperature boundary condition, the temperature profile along the radial direction is solely determined by the thermo conductivity and physical dimensions of the filling. Therefore, because the preset temperature differences among the lower six layers in the conic case shown in Fig. 5(b-2) are less than 20 °C, the temperatures at the tube centers can be maintained better than those in the constant-gradient case shown in Fig. 4(b-2), where the RMS errors are less than 2 °C for the lower six layers (averaged 1.4 °C). Because the preset temperatures at the top two layers have a 33 °C difference (i.e., 27 °C and 60 °C), the temperatures at the center are balanced in the middle with RMS errors of 10.1 °C and 2.3 °C, as shown in Fig. 5(b-2) and Table III. Similarly, because the preset temperature differences at the top and bottom regions in the experiment with the parabolic profile (shown in Fig. 6(b-2) and Table IV) are large, together with the edge transfer effect, the temperatures at the tube center have a larger discrepancy. If the filling in the tube is precious and should be completely utilized for analysis, one method to remedy this phenomenon is to add another two TE modules on both top and bottom of the incubator, which helps yield better environment control. If some of the filling can be included without post-analysis, the filling located around the top and bottom layers can be treated as the "buffer filling," which helps create an adequate surrounding temperature for the sample in the middle layers. The RMS steady-state temperature errors at the tube center in the middle six layers of the incubator with a parabolic profile are on average 3.9 °C.

The design and setup of the incubator is strongly constrained because the intrusion to the samples is undesirable in our designated applications. For applications where intrusions to the filling are permissible, the temperature sensors can be installed at the tube centers for feedback, such that the request temperature profiles at the centers can be adequately controlled and modulated. Nevertheless, in this scenario the temperatures at the tube surfaces will be inevitably higher than the request values because of heat transfer. Because our targeted application is to develop the incubator for anaerobic microbial incubation, the environment of the filling is strongly constrained. The sealing of the top cap is required to satisfy a certain sealing level, and the tube material (e.g., borosilicate glass) should be kept simple and inert to the filling. If temperature probing inside the incubator is adopted, a much more sophisticated and customized design for the test tube would be required. The present design with outer wall temperature feedback avoids such complexity. If the precise temperature control at the tube center is crucial, a temperature-mapping procedure can be utilized to find the empirical temperature distribution in-between the outer wall and the tube center before the experiments. Thus, the desired temperatures at the tube center can be achieved by correcting settings of the outer wall temperatures for the feedback control.

The dimensions of the test tube are determined by the balance of desired temperature profiles and required sample amount for post-analysis. As shown in Fig. 4 to Fig. 6, the temperature differences between the tube surface and center exist with the current tube diameter. If the precise one-dimensional temperature gradient in the vertical direction is crucial, a straightforward and quick solution to improve the performance of the present system is to decrease the tube diameter. This reduces the temperature variation between the tube wall and center caused by horizontal heat transfer. In this scenario, the transient and control performances will be improved as well because the heating capacity per unit filling increases with a decreasing tube radius. The simplified calculation is described as follows. Assume the radius of the tube is r and the height of each layer is h. The total heating capacity of one layer of the TE module is proportional to its surface (i.e., $2\pi rh$) and is responsible for heating the volume of the filling $\pi r^2 h$. Thus, the heating capacity per unit volume is inversely proportional to the radius r, so the tube with a small radius is preferred in the sense of temperature control. However, because there is a minimum amount of sample required for post-analysis, the volume of the filling $\pi r^2 h$ in each layer needs to be larger than a certain number. For example, for our typical acetate concentration analysis, the sampling volume of volcanic mud is around 1 cm^3. If a large volume is achieved by increasing the layer height, the temperature gradient in the vertical direction will be altered with flat zones because the TE module at each layer would try to even the temperature within the layer. Therefore, increasing the tube radius to enlarge the filling's volume seems to be the feasible solution. As a result, commercial borosilicate glass tubes with a diameter of 35 mm are chosen as the test tubes for the incubator. In this setup, the temperature drop across the radial direction of the test tube is inevitable because of the heat transfer. Although the temperature gradient is not perfectly aligned with the vertical direction, the gradient is still one dimensional because of the circular symmetry of the test tube. The shape of the constant temperature contour is not like flat disks but cone shaped. In the geo-environment, because the heat source is at the earth's center, the constant temperature contour in the macro-scale actually appears as a sphere, and the approximated vertical gradient results from the local viewpoint on a micro-scale. Therefore, the "perfectly" aligned temperature gradient in the vertical direction is not crucial as long as the contour of the one-dimensional gradient is known. Although the empirical temperature contour is basically determined by the heat transfer characteristics of the filling, which may vary significantly, the temperature variations from the surface to the center in the tube with different fillings have roughly similar trends unless the thermal conductivity is different in the large scale. Consequently, the experiments of the tube with quartz sand indeed provide the essential information of the empirical temperature profiles.

In principle, the idea of one-dimensional thermal modulation presented in this paper can be applied to various sizes of test tubes. As the tube diameter increases, the heat transfer in the radial direction increases. Thus, the maximum permissible tube diameter is determined by the tolerable temperature variation from the tube center to the preset temperature on the tube wall, which may vary and depends on the applications. On the other hand, as the tube size decreases, the amount of sample reduces. Thus, the minimum permissible tube diameter is determined by the required sample amount for the follow-up instrumental analysis, which may vary and depends on the applications as well. We found that a tube with a diameter of 35 mm has the adequate size in our application.

However, please note that the selected dimension is determined by our particular application, and different applications may yield different optimum tube dimensions.

IV. SUMMARY

We implement a novel, vertical temperature-mapping incubator using eight layers of TE modules mounted around a test tube to simulate the vertical temperature profile of desired geo-temperature variation with depth. We report the design considerations for the incubator, including spatial arrangement of the energy transfer mechanism, heating capacity of the TE modules, minimum required sample amount for follow-up analysis, and the constraint of non-intrusion to the geo-samples during incubation. Because of the last issue, the temperature on the tube wall is utilized for measurement feedback. The performance of the incubator is experimentally evaluated with two tube conditions (empty or filled with quartz sand) and under four preset temperature profiles (uniform, constant temperature gradient, monotonic-increasing parabolic, and parabolic). The experiment results show that, except for the top and/or bottom layers—which suffer from the edge heat transfer phenomenon—temperatures at the tube wall of the middle layers can be controlled with averaged RMS steady-state errors of 0.4 °C (empty tube) and 1.0 °C (filled tube). Because of the horizontal heat transfer, the temperatures at the tube center exhibit deviations from those on the tube wall, and the averaged RMS steady-state error is 2.7 °C (filled tube). The effect of edge heat transfer can be reduced by adding another TE module on the top and bottom of the incubator. Or, a more straightforward approach is to treat the filling around the top and bottom layers as a buffer and utilize filling in the middle layers for post-analysis. In principle, the idea of one-dimensional thermal modulation presented in this paper can be applied to various sizes of test tubes, and the optimum dimensions of the tube may differ depending on the applications.

ACKNOWLEDGMENTS

M.C.L., J.G.W., and M.F.T. are supported by Grant NSC 99-2815-C-002-082-E from the National Science Council (NSC) of Taiwan. The authors gratefully acknowledge the funding support from the NSC of Taiwan under Grant Nos. NSC 98-2627-M-002-015, NSC 99-2627-M-002-008, and NSC 100-2627-M-002-002. The authors would like to thank the National Instruments Taiwan Branch for the support of the equipment and technical consulting.

[1] M. Rasouli and L. S. J. Phee, Expert Rev. Med. Devices **7**(5), 693–709 (2010).
[2] D. Collins, E. Nesterenko, D. Connolly, M. Vasquez, M. Macka, D. Brabazon, and B. Paull, Anal. Chem. **83**(11), 4307–4313 (2011).
[3] R. F. Berg, Rev. Sci. Instrum. **82**(8) (2011).
[4] Y. Yang, F. C. Lin, and G. L. Yang, Rev. Sci. Instrum. **77**(6), 063701 (2006).
[5] R. K. Workman and S. Manne, Rev. Sci. Instrum. **71**(2), 431–436 (2000).
[6] X. S. Zhu, E. Krochmann, and J. S. Chen, Rev. Sci. Instrum. **63**(3), 1999–2003 (1992).
[7] N. Putra, A. W. Sukyono, D. Johansen, and F. N. Iskandar, Cryogenics **50**(11–12), 759–764 (2010).
[8] N. L. Gregory, T. D. W. Claridge, and M. Leonard, J. Magn. Reson. **124**(1), 228–231 (1997).
[9] H. T. Chua, A. Tay, and Y. Wang, J. Vac. Sci. Technol. B **27**(3), 1211–1214 (2009).
[10] T. Torfs, V. Leonov, and R. J. M. Vullers, Sens. Transducers **80**(6), 1230–1238 (2007).
[11] M. Mecke and F. Mensing, PTB-Mitt. **90**(6), 442–444 (1980).
[12] M. C. Liu, J. G. Wu, M. F. Tsai, W. S. Yu, P. C. Lin, I. C. Chiu, H. A. Chin, I. C. Cheng, Y. C. Tung, and J. Z. Chen, RSC Adv. **2**(4), 1639–1642 (2012).
[13] M. T. Madigan, J. M. Martinko, and J. Parker, *Brock Biology of Microorganisms*, 10th ed. (Prentice-Hall, New Jersey, 2000).
[14] D. S. Kelley, J. A. Karson, G. L. Fruh-Green, D. R. Yoerger, T. M. Shank, D. A. Butterfield, J. M. Hayes, M. O. Schrenk, E. J. Olson, G. Proskurowski, M. Jakuba, A. Bradley, B. Larson, K. Ludwig, D. Glickson, K. Buckman, A. S. Bradley, W. J. Brazelton, K. Roe, M. J. Elend, A. Delacour, S. M. Bernasconi, M. D. Lilley, J. A. Baross, R. T. Summons, and S. P. Sylva, Science **307**(5714), 1428–1434 (2005).
[15] K. Kashefi and D. R. Lovley, Science **301**(5635), 934–934 (2003).
[16] G. Eller, L. K. Kanel, and M. Kruger, Appl. Environ. Microbiol. **71**(12), 8925–8928 (2005).
[17] I. Sundh, C. Mikkela, M. Nilsson, and B. H. Svensson, Soil Biol. Biochem. **27**(6), 829–837 (1995).
[18] K. C. Condie, *Plate Tectpmocs amd Crustal Evolution* (Butterworth-Heinemann, 1997).
[19] J. M. Marques, J. E. Marques, P. M. Carreira, R. C. Graca, L. Aires-Barros, J. M. Carvalho, H. I. Chamine, and F. S. Borges, Geofluids **3**(3), 189–201 (2003).
[20] H. Niemann, T. Losekann, D. de Beer, M. Elvert, T. Nadalig, K. Knittel, R. Amann, E. J. Sauter, M. Schluter, M. Klages, J. P. Foucher, and A. Boetius, Nature (London) **443**(7113), 854–858 (2006).
[21] B. Ekstam and B. E. Bengtsson, Seed Sci. Technol. **21**(2), 301–308 (1993).
[22] J. Kallmeyer, T. G. Ferdelman, K. H. Jansen, and B. B. Jorgensen, J. Microbiol. Methods **55**(1), 165–172 (2003).
[23] W. H. Thomas, Am. J. Bot. **50**(6P2), 631 (1963).
[24] M. Suutari, K. Liukkonen, and S. Laakso, J. Microbiol. Methods **25**(3), 207–214 (1996).
[25] L. Elsgaard and L. W. Jorgensen, J. Microbiol. Methods **49**(1), 19–29 (2002).